

## PLANT PATHOLOGY AND NEMATODOLOGY

### Site-Specific Relationships between Cotton Root Rot and Soil Properties

C. D. Cribben, J. A. Thomasson\*, Y. Ge, C. L. S. Morgan, C. Yang, T. Isakeit, and R. L. Nichols

#### ABSTRACT

**Cotton Root Rot (CRR), caused by *Phymatotrichopsis omnivora*, is a problem across the southwestern United States and northern Mexico, commonly killing plants in infected portions of fields and greatly reducing overall yields. Over several decades a few studies have attempted to determine how soil properties influence the incidence of CRR, but no consistent associations have been found. Recent technological improvements allow for rapid collection of high-resolution disease damage estimates from aerial photography and of soil-property data, most notably with devices that measure apparent electrical conductivity (EC<sub>a</sub>). These technologies provide another avenue for evaluation of possible relationships between disease damage and soil properties. Data were collected from three geographically separated fields in Texas known to exhibit CRR: (1) aerial imagery to document CRR infection, (2) EC<sub>a</sub> data of soils with an electromagnetic induction device, and (3) several physical and chemical soil properties measured on soil cores sampled from the sites. Images were analyzed for incidence of CRR, and all other data were geographically overlaid for comparison among data sets. A significant relationship was found between EC<sub>a</sub> and CRR**

**at one site but was not found at the others. The relationship between EC<sub>a</sub> and other soil properties tended to involve hydrologic factors such as clay and sand contents, which affect soil water holding capacity, and depth to soil matrix effervescence and inorganic carbon content, which indicate relative water movement through the soil profile. Soil properties that were significantly related to CRR incidence included soil pH (two of three locations) and clay and sand contents (at one site only).**

Cotton Root Rot (CRR), caused by the fungus, *Phymatotrichum omnivora* (Duggar) Hennebert, has been a major cotton pathogen in the southwestern United States (mainly in Texas due to the many hectares of cotton grown there) and in northern Mexico since it was first described by Pammel (1888). From 2002 through 2011, roughly 6% of the Texas cotton crop was lost to this fungus on an annual basis (NCC, 2013). The disease tends not to infect entire fields (Lyda, 1978); instead each year it initiates shortly after flowering at specific, apparently conserved locations in a field and spreads in generally circular patterns from these foci (Uppalapati et al., 2010). The overwintering bodies of the fungus (sclerotia) lie dormant at various depths in the soil profile depending on soil type and location (Gerik, 1979). Though the fungus that causes CRR is soil-borne, only a few studies over many years have investigated soil properties associated with expression of the disease.

**Relation of Cotton Root Rot Incidence to Soil Properties.** Fraps and Fudge (1935) investigated the relationship between CRR incidence and the following soil properties on numerous soils across five regions in Texas: total and active phosphoric acid, nitrogen, total and acid-soluble potash, lime, basicity, and pH. Surface soils (0.00 to 0.18 m) and subsoils (0.18 to 0.48 m) associated with high levels of CRR damage tended to have higher active phosphoric acid, active potash, lime, basicity, and pH when compared to soils with healthy plants. The characteristics most closely related to CRR incidence were higher levels of lime and basicity.

---

Curtis Cribben, John Deere Turf Care, 6501 N.C. Highway 55, Fuquay-Varina, NC 27526; J.A. Thomasson\*, Department of Biological & Agricultural Engineering, Texas A&M University, 2117 TAMU, College Station, TX 77843; Y. Ge, Department of Biological Systems Engineering, University of Nebraska, P.O. Box 830726, Lincoln, NE, 68583; C.L.S. Morgan, Department of Soil & Crop Sciences, Texas A&M University, 545 Heep Center, College Station, TX 77843; C. Yang, Aerial Application Technology Research Unit, Agricultural Research Service, U.S. Department of Agriculture, 2771 F&B Road, College Station, TX 77845; T. Isakeit, Department of Plant Pathology and Microbiology, Texas A&M University, 2132 TAMU, College Station, TX 77843; and R.L. Nichols, Agricultural & Environmental Research, Cotton Incorporated, 6399 Weston Parkway, Cary, NC 27513

\*Corresponding author: [thomasson@tamu.edu](mailto:thomasson@tamu.edu)

Taubenhaus et al. (1937) conducted nine experiments to gauge the effect of soil acidity on the incidence of CRR using fine sandy loam, clay loam, and clay soils. In soils with pH from 4.0 to 8.0, it was generally seen that lower pH in the surface soil inhibited the fungus's ability to spread and overwinter. Results from smaller, more controlled experiments did not translate to the field scale in every case, and acidification of neutral soils appeared to be a temporary solution, as CRR incidence returned when the soil reverted to a neutral pH. It was also noted that acidification of highly calcareous soils is impractical at the field scale.

Lyda and Kissel (1974) observed the effects of exchangeable sodium levels in Houston black clay on CRR sclerotia formation. The total dry weight of sclerotia in cultures and the individual weights of sclerotia decreased as sodium saturation increased and as that of calcium decreased. Soil samples taken from fields infected with CRR verified these results.

Gerik (1979) collected soil cores from CRR-infected fields in various regions of Texas and Louisiana and measured extractable sodium, copper, manganese, zinc, chloride, pH,  $EC_w$  (electrical conductivity of the soil solution), bulk density and particle size distribution. Sodium was higher in non-infected areas at six of the 10 locations, but the differences were not statistically significant. At seven of the 10 locations there was also a tendency for pH to be higher in top layers of the non-infected soils, though this difference was not always significant. The soil  $EC_w$  also tended to be higher for non-infected areas at seven of the ten locations, although this trend was rarely statistically significant. There was no consistent relationship between particle size and CRR incidence, but bulk density was significantly higher for non-infected soils at almost all locations. Gerik (1979) also measured the quantity and depth of *P. omnivora* sclerotia. Excluding the Houston black soil from the Blackland Prairie region, in which sclerotia were abnormally deep, he found that soils had 59% of sclerotia in the top 0.30 m of soil.

Mueller et al. (1983) examined 13 CRR-infected southern-Arizona cotton fields for a relationship between CRR incidence and soil cations. The CRR infections were identified through infrared photography. Ninety soil cores were taken from infected and non-infected areas of the fields. In the majority of instances no significant difference was found in available and water-soluble sodium, potassium, calcium, or magnesium between the infected and non-

infected soils. Most notably, there were no instances in which infected soils had significantly higher sodium contents. Field tests were also performed with sodium chloride to mitigate the effects of CRR in ten field plots. Ground and aerial observations found no reduction in CRR incidence, and no significant differences in seed cotton yield or percent lint were seen between treated and untreated areas.

Smith and Hallmark (1987) investigated 26 historically CRR-infected fields in multiple regions of Texas including both Mollisols and Vertisols. Several physical and chemical soil properties were analyzed, such as particle size distribution, cation exchange capacity (with NaOAc), extractable bases, total carbon, pH (1:1 soil water ratio), soluble ions, calcium carbonate equivalent, bulk density, water content (-33 kPa tension), and the coefficient of linear extensibility. Each property was averaged to depths of 0.10, 0.50, and 1.0 m for statistical analysis. The only physical property with a significant difference between infected and non-infected areas was soil water content in the upper 0.50 m, and only in Blackland Prairie soils. A similar trend was found in Coastal Prairie soils, but the relationship was not statistically significant. Chemical properties that significantly differed in the Blackland and Coastal Prairies soils were extractable magnesium (to 0.50 and 1.0 m), the ratio of extractable calcium to magnesium (to 0.10, 0.50, and 1.0 m), and soluble bicarbonate (to 0.10 m). Significant chemical properties unique to the Blackland Prairie soils were the ratio of extractable potassium to magnesium (to 1.0 m), extractable iron (to 0.10 m), extractable zinc (to 0.50 m), and electrical conductivity (EC) (to 0.10 m). Significant chemical properties unique to Coastal Prairie soils were extractable copper (to 0.50 m) and soluble calcium (to 0.10, 0.50, and 1.0 m).

Matocha and Hopper (1995) performed several years of field studies in multiple southern Texas counties. Numerous paired samples of similar soils with and without CRR infection were collected and assessed for particle size. The CRR-infected soil had more sand and less clay than its paired counterpart. Additionally, the  $EC_w$ , sodium, calcium, and to a lesser extent potassium, were all higher for CRR infected soils. Water-extractable bicarbonate was generally higher for CRR infected soil, indicating a greater potential for carbon dioxide in the soil. Results also showed substantially lower manganese and zinc levels and slightly lower iron and copper levels in CRR-infected soils, all chemical properties associated with high pH soils.

While there is commonality among these studies, overall the results suggest that the relationship between soil properties and CRR incidence is weak. Multiple soil properties may be involved, and relationships may vary among regions. Recent innovations in soil-property data collection from the field, such as with mobile soil  $EC_a$  sensors, can enable analysis of larger data sets and possibly reveal clearer and more consistent relationships between CRR incidence and soil properties.

**EC<sub>a</sub> Theory and Uses.** Some of the soil properties associated with CRR in the literature were pH, EC, moisture, calcium, exchangeable sodium, zinc, iron, copper, extractable bicarbonates, and bulk density. A few of these are associated with bulk soil EC measurements (Corwin et al., 2003). Rhoades et al. (1976) rigorously modeled the interaction of soil EC, soil water salinity, and other related soil properties. Their data fit Equation 1 as long as volumetric water content ( $\theta$ ) was above a critical value.

$$EC_a = EC_w \theta T + EC_s \quad (1)$$

$EC_a$  is the sum of the bulk surface conductivity ( $EC_s$ , related to ions at the soil-water interface) and the bulk liquid-phase conductivity ( $EC_b$ , related to free salts in the soil solution), which is the product of  $EC_w$ ,  $\theta$ , and the transmission coefficient ( $T$ ). Rhodes et al. (1976) suggested that some terms of the model could be estimated based on soil properties, allowing for testing outside of reference water contents such as field capacity.

Bulk  $EC_a$  can be measured proximally in the field by two fast and reliable methods, direct contact and electromagnetic induction (EMI). Corwin and Lesch (2003) describe the methods and their advantages in precision-agriculture applications. Direct contact methods use at least four electrodes in good physical contact with the soil (Lund et al., 1999), while the EMI method uses two coils at a fixed distance; one acts as a transmitter and the other a receiver. Alternating current is passed through the transmitter coil, generating a magnetic field of alternating direction in the soil. The changing orientation of the magnetic field induces a current in the soil that generates a secondary magnetic field. The amplitude and phase of the secondary magnetic field is measured by the receiver coil and subsequently compared to the transmitter signal. The amplitude and phase difference of the two signals is related to soil  $EC_a$ . The vertical and horizontal dipoles on one EMI instrument, the EM38DD (Geomatrix Earth

Science Ltd, Bedfordshire, UK), can measure soil  $EC_a$  to depths of 1.5 and 0.75 m, respectively (McNeill, 1992). Advantages of EMI include reduced measurement variability due to the large amount of soil involved and the ability to measure dry or rocky soils without contact issues (Hendrickx et al., 2002).

In well-drained, non-saline, agricultural fields,  $EC_a$  measurements can be expected to correlate with soil properties associated with texture and water content. A variety of agricultural practices employ an EMI device for data collection. Triantafyllis and Lesch (2005) used EMI to map clay content in Australian fields. Kachanoski et al. (1988) studied an area in Ontario, Canada, with low levels of soluble salts to determine relationships between soil  $EC_a$ ,  $\theta$ , and soil texture. They found that soils across a wide range of textures with low levels of soluble salts have  $EC_a$  values that are correlated to soil water content. Other soil properties such as depth to clay pan (Kitchen et al., 2003) and soil herbicide partitioning coefficient (Jaynes et al., 1995) have been successfully measured with  $EC_a$  in well-drained non-saline soils.

**Objectives.** The literature and preliminary work in this study suggest that  $EC_a$  could potentially be used as a predictor of CRR-infection locations. The objectives of this study were thus (1) to determine the relationship between soil  $EC_a$  and CRR incidence in selected fields, (2) to quantify the relationship between soil  $EC_a$  and various other soil properties of interest, and (3) to examine the various other soil properties for relationships to CRR incidence.

## MATERIALS AND METHODS

**Site Description.** Three locations across the state of Texas with established histories of CRR were chosen for this study. Site 1 (GPS coordinates: 30.604201, -97.287416) is a non-irrigated, 2.8 ha (6.8 ac) field located near Thrall, Texas, in the Northern Blackland Prairies, and is cropped in a year-to-year cotton-corn rotation. The soils in the field are mapped as Burleson clay (fine, smectitic, thermic Udic Haplusterts) and Branyon clay (fine, smectitic, thermic Udic Haplusterts). Both series consist of very deep, moderately to well drained, very slowly permeable soils. Burleson soils formed from alkaline sediments, whereas Branyon soils formed from calcareous sediments.

Sites 2 and 3 are both drip irrigated. Site 2 (28.143053, -97.702267), located near Sinton, Texas, in the Southern Subhumid Gulf Coastal Prairies,

covers 9.1 ha (22.6 ac) and is in cotton monoculture. The soils are mapped as Edroy clay (fine, smectitic, hyperthermic Ustic Epiaquerts), Orelia fine sandy loam and sandy clay loam (fine-loamy, mixed superactive, hyperthermic Typic Argiustolls). Edroy clay is very deep, poorly drained, and very slowly permeable, while Orelia is very deep, well drained, and slowly permeable. The soils formed from loamy fluviomarine deposits.

Site 3 (31.442904, -100.374961), located near San Angelo, in the Red Prairies region of Texas, covers 6.0 ha (14.8 ac) and is also in cotton monoculture. The soils are mapped as Angelo clay loam (fine-silty, mixed superactive, thermic Aridic Calciustolls) and Mereta clay loam (clayey, mixed, superactive, thermic, shallow Petrocalcic Calciustolls). Angelo clay loam is deep or very deep, well drained, and moderately slowly permeable. Mereta clay loam is shallow (0.48 to 0.58 m) to a petrocalcic horizon, and well drained. The soils in this field formed from calcareous alluvium.

**Aerial Imagery Collection.** Incidence of CRR for each field was determined with aerial imagery. The images were captured at an above ground level (AGL) altitude of 2438 m with a multispectral digital-imaging system described by Yang (2012). Pixel resolution was approximately 0.75 m. Four cameras were each equipped with an optical filter to create images from the blue, green, red, and near-infrared spectral bands. One aerial image at Site 1 was collected each growing season from 2010 through 2012, corresponding to 107, 86, and 146 days after planting (DAP), respectively. An image of Site 2 was collected in 2010 and 2011 at 124 and 120 DAP, respectively. For Site 3, one image was collected in 2010 (105 DAP), two in 2011 (126 and 138 DAP) and three in 2012 (97, 108, and 122 DAP).

**EC<sub>a</sub> Data Collection.** An EC<sub>a</sub> survey was performed at each location between the 2010 and 2011 growing seasons with an EM38DD, which was pulled inside a wooden sled behind an all-terrain vehicle. Measurements of EC<sub>a</sub> were recorded in millisiemens per meter (mS/m), corrected to 25°C (EC<sub>25</sub>) (Ma et al., 2010), and logged at 1.0-s intervals with both the vertical and horizontal dipoles. Transects of each field were made approximately 4.5 m apart to maximize map resolution. A WAAS-capable GPS unit (Trimble Navigation Limited, Sunnyvale, CA) was used to spatially reference the data. Surveys of EC<sub>a</sub> at all three sites were conducted during

the winter months when the fields were fallow. It is therefore reasonable to assume that soil moisture would have been near field capacity when the data were collected. The data were imported into ArcGIS (ESRI, Redlands, CA) in order to map the soil EC<sub>a</sub> and relate it to features in the aerial images.

**Soil Core Collection.** Soil cores were collected from pre-defined strata within all three sites after the 2011 growing season. The vertical EC<sub>a</sub> measurements (mS/m) at each site were split into three equal-sized categories representing the low, medium, and high thirds of EC<sub>a</sub> measurements taken at the given site:

Site 1 < 75, 75 - 90, > 90

Site 2 < 58, 58 - 87, > 87

Site 3 < 57, 57 - 69, > 69.

Six strata were thus defined at each site as low EC<sub>a</sub> and healthy plants, low EC<sub>a</sub> and infected plants, medium EC<sub>a</sub> and healthy plants, medium EC<sub>a</sub> and infected plants, high EC<sub>a</sub> and healthy plants, and high EC<sub>a</sub> and infected plants. Soil cores were collected from each of the six strata with a soil coring truck equipped with a Giddings Probe (Giddings Machine Company, Windsor, CO). At Site 1, six total soil cores were taken to a depth of approximately 1.6 m unless obstructions prohibited the probe from going deeper. The twenty-three soil cores collected at Site 2 were taken down to the soil parent material giving an average core depth of 1.4 m. Twenty-two soil cores were collected at Site 3 to the depth of dense calcic horizon or parent material, resulting in an average core depth of 1.1 m. All cores were collected in plastic sleeves, which were capped and transported to the laboratory for analysis.

**Soil Core Analysis.** The depth at which the soil matrix had free carbonates was noted by testing for effervescence with 1 N hydrochloric acid. The depth at which secondary calcium carbonate concentrations began appearing in the soil was also noted. Next, each soil core was cut in half lengthwise and described by horizon and assigned horizon nomenclature. A subsample of soil was collected from each horizon for subsequent laboratory analysis. The samples were air dried at 60°C and then ground and passed through a 2-mm sieve. The remaining soil analyses were performed on each horizon of every soil core. Particle size analysis was conducted with the pipette method as described by Kilmer and Alexander (1949). The inorganic carbonates were measured with the modified pressure-calciometer method

(Sherrod et al., 2002). Soil pH and EC were both tested on a 1:1 water-soil mixture with a pH meter and an EC meter at the Texas A&M Agrilife Research Soil Characterization Laboratory. Soil properties were averaged by depth in increments of 10, 20, and 30 cm down to the parent material. Depth-weighted averages allowed for a more straightforward comparison between soil cores, because horizon depths were not uniform across all cores.

**Data Analysis Techniques.** Statistical analysis began with directly comparing  $EC_a$  measurements to CRR incidence. The normalized difference vegetation index (NDVI) was calculated on a pixel-by-pixel basis within each image and used to estimate the ground coverage of CRR, which was assumed to be the major source of crop canopy damage in the field. The CRR-infected plants were either wilted or desiccated at the time of image collection, resulting in clear differences in NDVI between infected and non-infected areas. Each field NDVI image was overlaid with a 15 by 15 m grid (Site 2, 359 grid cells) or 12 by 12 m grid (Sites 1 and 3, 185 and 359 cells, respectively). An average  $EC_a$  and NDVI measurement for each cell was calculated (figure 1), and the correlation between the two was calculated with Ordinary Least Squares (OLS) regression.

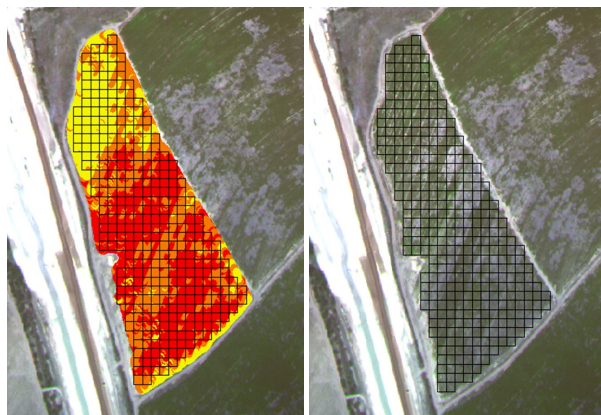


**Figure 1.** Site 3  $EC_a$  map (left) and remotely sensed image (right) overlaid with grid for calculation of average  $EC_a$  and NDVI measurement for each cell.

Next, the other measured soil properties were compared to  $EC_a$  to discern which factors were influencing  $EC_a$  variability. All measurement data were included in a multi-factor analysis. The REG-SUBSETS function in the R statistical software package (R Development Core Team, Vienna, Austria) was used to analyze the data. This function selected the most significant soil properties and

created multiple linear regression (MLR) models that would account for the most variance in the soil  $EC_a$  measurements. Soil properties included in the MLR analysis were depth of the soil A horizon, depth to soil matrix effervescence, depth to the presence of calcium carbonate nodules, and the weighted averages of pH, EC, clay, sand, and inorganic carbon content.

Finally, t-tests were performed to identify significant soil property differences between soil cores taken from healthy and CRR-infected areas, which were delineated with the NDVI images. Since the CRR fungus tends to reside for long periods of time in the same field areas, one NDVI image from each field was selected as showing the fullest expression of CRR in the field. These NDVI images were classified into healthy and infected regions by visual assessment. Soil properties included in the t-test analysis were the same as those considered in the MLR analysis. There were concerns about spatial autocorrelation that might exist among soil cores, in particular for those with small separation distance. Therefore, semivariogram analysis was performed on the  $EC_a$  data to evaluate the degree of spatial autocorrelation at each site. An empirical semivariogram of  $EC_a$  was created for each of the fields, and the lag distance was identified.

## RESULTS AND DISCUSSION

**Soil  $EC_a$  versus CRR Incidence.** The OLS regression analysis between  $EC_a$  and NDVI for each grid cell produced a significant ( $p < 0.0001$ ) linear trend with an  $R^2$  value of 0.37 for Site 3 (figure 2), indicating that 37% of the variability in CRR incidence (considering NDVI as a proxy) could be explained by variability in  $EC_a$ . However, while the other sites also had statistically significant trends ( $p < 0.01$  for Site 1;  $p < 0.001$  for Site 2), neither Site 1 ( $R^2 < 0.01$ ) nor Site 2 ( $R^2 = 0.03$ ) had a strongly explanatory relationship between CRR and  $EC_a$ . These low  $R^2$  values imply that soil  $EC_a$  cannot be used directly to map CRR incidence, but the presence of a moderate relationship is apparent in some instances. The literature indicates that soil moisture and clay content relate strongly to  $EC_a$  (Corwin et al., 2003) and to some extent to CRR (Smith and Hallmark, 1987; Gerik, 1979; Matocha and Hopper, 1995), corroborating the moderate relationship observed between soil  $EC_a$  and CRR incidence at one of three sites.

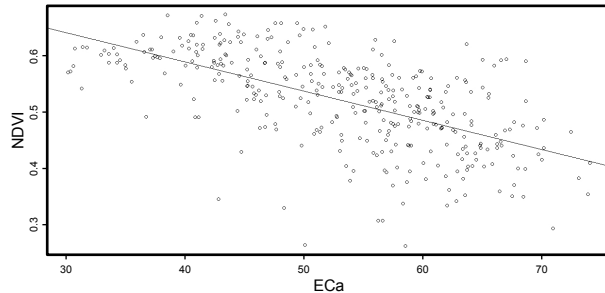


Figure 2. Relationship between  $EC_a$  (mS/m) and NDVI at Site 3.

**Soil  $EC_a$  Measurements versus Other Soil Properties.** Results of soil coring indicated that, in general, the soils at Site 1 are comprised of 40 to 60% shrink-swell clays and have a thick (up to 2 m) solum. Soil properties that best explained the variability in  $EC_a$  at each location are shown in table 1. Data from Site 1 exhibited a strong positive relationship between  $EC_a$  and depth to soil matrix effervescence and between  $EC_a$  and clay content from 50 to 60 cm. Because of the limited number of soil cores taken at Site 1, only single-regressor models were considered for that location. The temperature-corrected  $EC_{25}$  map, aerial image, and coring locations for Site 1 are shown in figure 3.

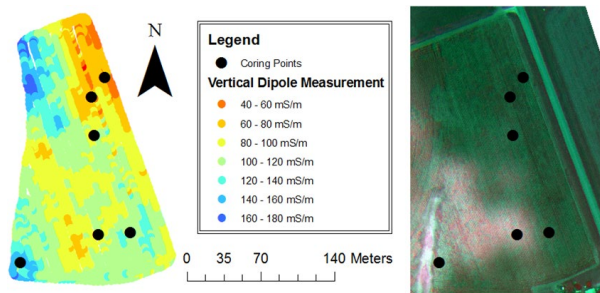


Figure 3. The  $EC_{25}$  ( $EC_a$  corrected to 25°C) map of Site 1 (near Thrall, TX) shown side by side with the remote sensing aerial image taken on 8/11/2010 with the location of soil coring points superimposed on both.

Site 2 soils also had a very thick (up to 2 m) solum, and notable clay and calcium carbonate accumulations were observed around 25 and 76 cm deep, respectively. The strongest relationship between  $EC_a$  and other soil properties observed at Site 2 was a positive correlation with clay content at 50 to 60 cm deep and depth to soil matrix effervescence. Two-regressor models were the largest considered for Site 2, because any additional regressor was not significant at the  $\alpha=0.05$  level. The  $R^2$  values for these models were much lower than those for Site 1 (Table 1). The temperature corrected  $EC_{25}$  map, aerial image, and coring locations for Site 2 can be seen in figure 4.

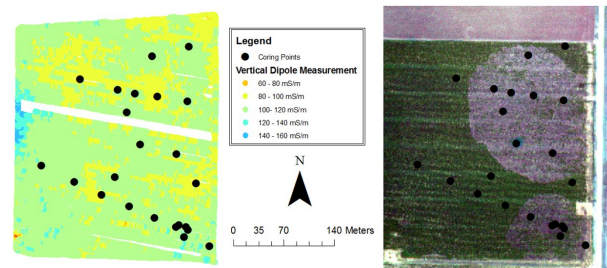


Figure 4. The  $EC_{25}$  ( $EC_a$  corrected to 25°C) map of Sinton shown side by side with the remote sensing aerial image taken on 7/7/2011 with the location of soil coring points superimposed on both.

Site 3 soils exhibited a petrocalcic horizon around 50 cm deep, and the soil matrix effervesced to the surface. The petrocalcic horizon is comprised of a strongly cemented layer of calcium carbonate (Bkm) and can inhibit rooting depth in the soil. Analyses of Site 3 soil-property data produced models of one, two, and three significant terms that could explain up to 84% of the variability seen in the soil  $EC_a$  measurements. There was a positive relationship between  $EC_a$  and depth of clay content and inorganic carbon (calcium carbonate) concentrations. The temperature corrected  $EC_{25}$  map, aerial image, and coring locations for Site 3 can be seen in figure 5.

Table 1. Multiple linear regression results for  $EC_a$  and soil property data at each location

Location	Number of Regressors in model	Regressor 1	Regressor 2	Regressor 3	Model $R^2$
Site 1	1	(+) Matrix Eff. <sup>[z]</sup>			0.78
Thrall, Texas	1	(+) Clay <sup>[y]</sup> 50-60 cm			0.72
Site 2	1	(+) Clay <sup>[y]</sup> 50-70 cm			0.16
Sinton, Texas	2	(+) Clay <sup>[y]</sup> 50-60 cm	(+) Matrix Eff. <sup>[z]</sup>		0.34
Site 3	1	(+) Clay <sup>[y]</sup> 20-40 cm			0.52
San Angelo, Texas	2	(+) Clay <sup>[y]</sup> 15-45 cm	(-) Sand <sup>[x]</sup> 50-60 cm		0.75
	3	(+) Clay <sup>[y]</sup> 45-75 cm	(-) Sand <sup>[x]</sup> 15-45 cm	(+) IC <sup>[w]</sup> 70-90 cm	0.84

<sup>[z]</sup> Matrix Eff. The depth at which the soil matrix effervesced when in contact with HCl.

<sup>[y]</sup> Clay The percent clay content of the soil at the specified depth.

<sup>[x]</sup> Sand The percent sand content of the soil at the specified depth.

<sup>[w]</sup> IC The inorganic carbon content of the soil in grams per kilogram at the specified depth.

(+/-) Indicates whether the term is positive or negative in the model.

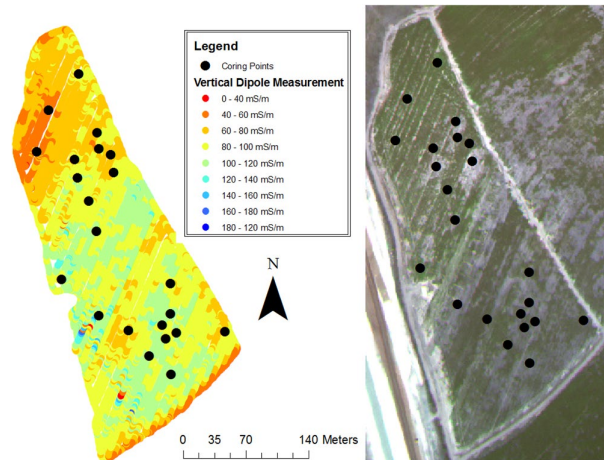


**Figure 5.** The EC<sub>25</sub> (EC<sub>a</sub> corrected to 25°C) map of San Angelo shown side by side with the remote sensing aerial image taken on 8/23/2010 with the location of soil coring points superimposed on both.

The results across all three locations are supported by observations in previous research. Higher soil clay contents correspond to larger water holding capacities, and soil moisture and clay content are factors that influence EC<sub>a</sub> (Corwin et al., 2003). The negative correlation between EC<sub>a</sub> and sand content was to be expected due to sand’s poor water-holding capabilities. The data in table 1 also suggest that calcium carbonate levels were related to EC<sub>a</sub> through the soil properties of inorganic carbon content and soil matrix effervescence.

**Other Soil Properties versus CRR Incidence.**

Soil-core properties at Sites 2 and 3 that were significantly different between healthy and CRR-infected areas are shown in table 2. The pH values listed in the

table are given only to the tenth’s place, because there was concern about their level of precision, but values to the hundredth’s place were used in the analysis. For each property presented, its depth, average value for soils with healthy plants, and average value for soils with symptomatic plants is listed. In the analysis of spatial autocorrelation, the distance between core-sample locations was generally greater than the lag distance identified in each semivariogram, suggesting that the sampling points were beyond the spatial autocorrelation distance of the soil properties studied. Therefore, it was reasoned that the influence of spatial autocorrelation on the validity of the pooled t-tests should be minimal. The purpose of the pooled t-tests was to determine whether there were significant differences in particular soil properties between healthy and CRR-infected areas. Site 1 had no significant soil properties at the  $\alpha=0.05$  level due at least in part to the small data set being evaluated. Site 2 did have significant differences in clay, sand, inorganic carbon, and pH at varying depths. It is not surprising that the soil texture properties of clay and sand were significant at similar depths due to their relation to each other. The Site 2 pH relationships are in agreement with Gerik (1979) in that healthy plants were associated with soils of higher pH values. However, this result was in disagreement with the pH relationships seen by Fraps and Fudge (1935) and Taubenhaus et al. (1937). Additionally, the majority of differences seen at Site 2 were in the top 30 cm of soil, also in agreement with the finding of Gerik (1979). The role of inorganic carbon content as it relates to CRR is unknown.

**Table 2.** Soil-core properties at Sites 2 and 3 that were significantly different ( $\alpha=0.05$ ) between healthy and CRR-infected areas; no significant differences existed at Site 1. Average values of the significant soil factors in the healthy and infected soils are listed according to Site and depth in the soil core. The pH values are given only to the tenth’s place, because there was concern about their level of precision, but values to the hundredth’s place were used in the analysis

Site 2 (n=23: 11 Healthy, 12 Infected)										Site 3 (n=22: 12 Healthy, 10 Infected)					
Clay (%)			Sand (%)			Inorganic Carbon (g/kg)			pH		pH				
Depth (cm)	Healthy	Infected	Depth (cm)	Healthy	Infected	Depth (cm)	Healthy	Infected	Depth (cm)	Healthy	Infected	Depth (cm)	Healthy	Infected	
0-10	28.1	24.9	0-10	56.5	59.0	90-100	8.0	11.5	0-10	7.0	6.2	0-10	7.8	7.7	
10-20	28.1	25.0	10-20	56.5	58.9				10-20	7.0	6.3	10-20	7.8	7.7	
0-20	28.1	24.9	0-20	56.5	58.9				0-20	7.0	6.3	20-30	7.8	7.7	
10-30	28.2	25.6	10-30	56.4	58.6				10-30	7.0	6.4	0-20	7.8	7.7	
									0-30	7.0	6.4	10-30	7.8	7.7	
												20-40	7.8	7.8	
												0-30	7.8	7.7	
												15-45	7.8	7.8	

The significant differences at Site 3 were only in pH and were at depths similar to those at Site 2. Also the same pattern of higher pH values associated with healthy soils was observed. The pH measurements for Site 3 were very consistent (often identical in the tenth's place), and the lack of overall spread in the data allowed the small differences (in the hundredth's place) to be significant. The consistency in pH values at Site 3 suggests the relationship between pH and CRR at Site 3 may not be as clearly defined as at Site 2. This lack of spread in the data is particularly clear for the Site 3 pH values from 15 to 45 cm, where rounding to the nearest tenth resulted in the same reported value for both healthy and infected regions.

**Conclusion.** In summary, a moderate relationship was found between EC<sub>a</sub> and CRR at one site, but this relationship did not exist at the other sites. The relationship between EC<sub>a</sub> and other soil properties involved hydrologic factors such as clay and sand contents (which relate to soil water holding capacity), and depth to soil matrix effervescence and inorganic carbon content (which relate to water movement through the soil profile). Soil properties that were significantly related to CRR incidence included soil pH (a finding consistent across two locations) as well as clay and sand contents (at one site only). In some instances the results of this study have corroborated findings of previous research, and in one respect these results agree with the entirety of previous literature on the subject: the relationship between soils and CRR is complex, inconsistent, and not strong enough to enable using soil properties as a predictor for CRR location.

#### **Practical Implications and Future Research.**

The measurement of EC<sub>a</sub> has become commonplace on research farms and commercial farms employing precision agriculture. If measurements are made appropriately, the data provide a lasting map of important soil variability within a field. Maps of EC<sub>a</sub> are used in decision making regarding fertilizer application, irrigation, and seeding rate, to name a few applications. If it were determined that EC<sub>a</sub> could be used along with other variables to predict CRR locations, new mitigation strategies could potentially be developed. The scope of this study was limited to soil properties, but researchers in future studies may wish to consider other variables as well. For example, topographic properties such as elevation, slope, and aspect may influence CRR infection. Another vari-

able that could be considered is the time during the growing season about which the differentiation is made between healthy and CRR-infected crop. Since CRR tends to show up at a few small spots that then merge together into larger spots, it is conceivable that relationships between soil properties and current CRR incidence would show up at earlier times than when CRR is fully expressed.

### **ACKNOWLEDGEMENTS AND/OR DISCLAIMERS**

Financial support for this work has been provided by Cotton Incorporated and the Texas State Support Committee.

### **REFERENCES**

- Corwin, D.L., S.R. Kaffka, J.W. Hopmans, Y. Mori, J.W. van Groenigen, C. van Kessel, S.M. Lesch, and J.D. Oster. 2003. Assessment and field-scale mapping of soil quality properties of a saline-sodic soil. *Geoderma* 114: 231-259.
- Corwin, D.L., and S.M. Lesch. 2003. Application of soil electrical conductivity to precision agriculture: theory, principles, and guidelines. *Agron. J.* 95:455-471.
- Frap, G.S., and J.F. Fudge. 1935. Relation of the occurrence of cotton root rot to the chemical composition of soils. *Texas Agric. Exp. Station Bulletin No.* 545.
- Gerik, J.S. 1979. Vertical distribution of sclerotia of *Phytophthora omnivorum* (Shear) Duggar relative soil chemical and physical properties. M.S. Thesis. College Station, Texas: Texas A&M University, Department of Plant Pathology.
- Hendrickx, J.M.H., B. Borchers, D.L. Corwin, S.M. Lesch, A.C. Hilgendorf, and J. Schlue. 2002. Inversion of soil conductivity profiles from electromagnetic induction measurements: theory and experimental verification. *Soil Sci. Soc. Am. J.* 66:673-685.
- Jaynes, D.B., J.M. Novak, T.B. Moorman, and C.A. Cambardella. 1995. Estimating herbicide partition coefficients from electromagnetic induction measurements. *J. Environ. Qual.* 24:36-41.
- Kachanoski, R.G., E.G. Gregorich, and I.J. Wesenbeeck. 1988. Estimating spatial variations of soil water content using noncontacting electromagnetic inductive methods. *Can. J. Soil Sci.* 68:715-722.
- Kilmer, V.H., and L.Z. Alexander. 1949. Methods for making mechanical analyses of soils. *Soil Sci.* 68: 15-24.

- Kitchen, N.R., S.T. Drummond, E.D. Lund, K.A. Sudduth, and G.W. Buchleiter. 2003. Soil electrical conductivity and topography related to yield for three contrasting soil-crop systems. *Agron. J.* 95:483-495.
- Lund, E.D., C.D. Christy, and P.E. Drummond. 1999. Practical applications of soil electrical conductivity mapping. In *Proc 2<sup>nd</sup> European Conf. Precision Agric.*, 771-779. J.V. Stafford, ed. Sheffield, UK: Sheffield Academic Press.
- Lyda, S.D. 1978. Ecology of *Phymatotrichum omnivorum*. *Ann. Rev. of Phytopathol.* 16: 193-209.
- Lyda, S.D., and D.E. Kissel. 1974. Sodium influence on disease development and sclerotial formation by *Phymatotrichum omnivorum*. In *Proc. of the American Phytopathol. Soc.*, 163-164. St. Paul, Minn.: APS Press.
- Ma, R., A. McBratney, B. Whelan, B. Minasny, and M. Short. 2010. Comparing temperature correction models for soil electrical conductivity measurement. *Precision Agric.* 12:55-66.
- Matocha, J.E., and F.L. Hopper. 1995. Influence of soil properties and chemical treatments on *Phymatotrichum omnivorum* in cotton. In *1995 Proc. Beltwide Cotton Conf. Proc.*, 224-232. Cordova, Tenn.: National Cotton Council.
- McNeill, J.D. 1992. Chapter 11: Rapid, accurate mapping of soil salinity by electromagnetic ground conductivity meters. In *Advances in Measurement of Soil physical Properties: Bringing Theory into Practice*, 209-229. G.C. Topp, W.D. Reynolds, and R.E. Green, eds. Madison, Wisc.: SSSA.
- Mueller, J.P., R.B. Hine, D.A. Pennington, and S.J. Ingle. 1983. Relationship of soil cations to the distribution of *Phymatotrichum omnivorum*. *Phytopathol.* 73(10): 1365-1368.
- NCC. 2013. Disease Database 2011. Cordova, TN: National Cotton Council of America. Available at: <http://www.cotton.org/tech/pest/index.cfm>. Accessed 20 February 2013.
- Pammel, L.H. 1888. Root Rot of Cotton, or "Cotton blight". Texas Agric. Exp. Station Ann. Report 1: 50-65.
- R Development Core Team. 2011. R: A language and environment for statistical computing. R Foundation for Statistical Computing, Vienna, Austria. ISBN 3-900051-07-0, URL <http://www.R-project.org/>.
- Rhoades, J.D., P.A.C. Raats, and R.J. Prather. 1976. Effects of liquid-phase electrical conductivity, water content, and surface conductivity on bulk soil electrical conductivity. *Soil Sci. Soc. Am. J.* 40:651-655.
- Sherrod, L.A., G. Dunn, G.A. Peterson, and R.L. Kolberg. 2002. Inorganic carbon analysis by modified pressure-calimeter method. *Soil Sci. Am. J.* 66: 299-305.
- Smith, R.B., and C.T. Hallmark. 1987. Selected chemical and physical properties of soils manifesting cotton root rot. *Agron. J.* 79: 155-159.
- Taubenhaus, J.J., W.N. Ezekiel, and J.F. Fudge. 1937. Relation of soil acidity to cotton root rot. Texas Agric. Exp. Station Bulletin No. 545.
- Triantafyllis, J., and S.M. Lesch. 2005. Mapping clay content variation using electromagnetic induction techniques. *Comput. Electron. Agr.* 46: 203-237.
- Uppalapati, S.R., C.A. Young, S.M. Marek, and K.S. Mysore. 2010. *Phymatotrichum* (cotton) root rot caused by *Phymatotrichopsis omnivora*: retrospects and prospects. *Molecular Plant Pathol.* 11(3): 325-334.
- Yang, C. 2012. A high-resolution airborne four-camera imaging system for agricultural remote sensing. *Comput. Electron. Agr.* 88: 13-24.